JOURNAL OF MATERIALS SCIENCE 23 (1988) 4517–4520

A practical classification of ferromagnets in relation to composition, temperature and fabrication process variations

C. Y. TAY
Department of Metallurgy and Materials, University of Birmingham, PO Box 363, Birmingham, B15 2TT, UK

The classification of sets of ferromagnets may be usefully discussed in a graphical form by plotting the H_{cB}/B_r and H_{cI}/B_r ratios of the individual magnets. For each set, a curve of the form $H_{cB}/B_r = K(H_{cI}/B_r)^L$, can be fitted, where K and L are constants of fit. This general form is discussed in detail with respect to the theoretical limiting cases. An appraisal of data from several sets of rare earth-based ferromagnets indicates that these ferromagnetic materials can be classified into three general types, especially when the powder metallurgical processes and conditions for fabricating the actual magnets are taken into consideration. Effects of composition and temperature variations on the magnetic properties can also be consistently discussed within this classification.

1. Introduction

We have recently shown [1, 2] that when the H_{cI}/B_r and H_{cB}/B_r ratios (hereafter these may be more concisely referred to as X and Y respectively) of individual magnets which form a defined set are plotted a characteristic curve is obtained. Ferromagnets form a set when the following conditions are satisfied: (a) they are of basically the same, or similar material composition; (b) they are produced by the same fabrication route and (c) they have been subjected to similar environmental conditions. The initial basis for plotting these ratios stems from an empirical classification of ferromagnets into two types according to the Becker conditions [3]. In cgs units these are given as: type 1: $X \sim Y \ll 1$ and type 2: $X \gg Y \sim 1$ (cgs units are preferred as the unity factors in both conditions are, less conveniently, replaced by $(1/0.4\pi)$ in SI units). The implications and usefulness of the Becker conditions are enhanced through the graphical (X, Y) representation since it allows the treatment of individual magnets to be replaced by that of sets of magnets.

This paper first discusses the need for a third type of ferromagnet which is specified by a condition intermediate between the original Becker conditions. The different forms of the $Y = KX^L$ equation which arise according to the various possible combinations of the constants of fit, K and L, are then identified and correlated to the different types of magnets with the aid of empirical data from several typical sets of rare earth-based magnets. Finally, we examine the possible extension of the (X, Y) graph scheme for categorizing the effects of magnet fabrication processes and conditions, as well as, compositional and temperature variations.

2. The classification of ferromagnet sets

2.1. A third type of ferromagnet

The Becker conditions [3] classify ferromagnets into two types according to their demagnetization characteristics. A Type I ferromagnet is characterized by a high remanence (B_r) but relatively much lower coercivities (H_{cI} and H_{cB}). Hence this type of magnet is deficient in $(BH)_{max}$ products and also easily demagnetized. In contrast, the more recently developed RE-based magnets are classified as type 2 because they show promise of high B_r and extremely high H_{cI} values. They therefore have almost ideally square demagnetization loops and high $(BH)_{max}$ products. However, attempts at fabricating practical magnets from type 2 materials have encountered various problems which prevent the realization of their ideal properties. This situation suggests that the Becker classification may not be comprehensive and that a third type (which we shall call type T) can be distinguished to permit a smooth transition between types 1 and 2.

The condition corresponding to the type T ferromagnets is of the form $X \geqslant Y \sim 1$, which clearly falls between the two Becker conditions. Thus type T magnets may be characterized by high remanences and comparable coercivities whereas type 2 magnets may also have high remanences but are more especially marked by the possibility of possessing extremely high H_{cI} values (in excess of both B_r and H_{cB}).

2.2. The (X, Y) graph for ideal ferromagnets

For the square demagnetization loops of ideal ferromagnets the approximate equalities in all the three magnet type classification conditions become

0022–2461/88 $03.00 + .12

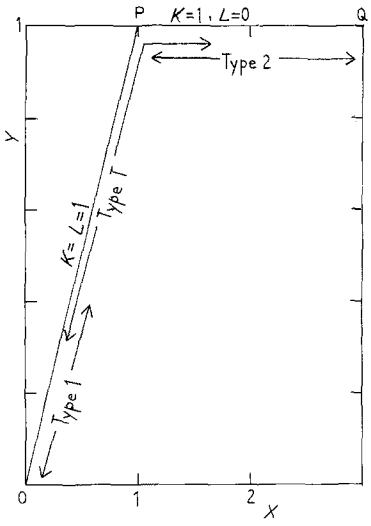

Figure 1 A schematic representation of the (X, Y) ranges for the proposed types (1, T and 2) of ferromagnet sets.

equalities. These magnets are then represented on the (X, Y) graph by points lying on either of the lines OP and PQ shown in Fig. 1. The line OP has constant unity gradient while the line PQ represents constant unity Y value (zero gradient). The lower $X = Y$ values on OP correspond to type 1 while the higher values correspond to type T ideal magnets. Similarly, the lower X values on the PQ line may be considered as corresponding to type T and the higher values to type 2 magnets. In each of these cases the changeover from one type to another is not abrupt but occupy a range of mixed type characteristics. The point P is especially interesting as it is the intersection of OP and PQ which involves an abrupt change of gradient from 1 to 0.

2.3. The (X, Y) graph for fabricated magnets

A smooth curve of the form $Y = KX^L$ can be fitted [1, 2] to the plotted (X, Y) data for a set of fabricated magnets. This curve replaces and reduces to the lines OP ($K = L = 1$) and PQ ($K = 1$, $L = 0$) for ideal magnets. In addition, the point P, at which there is an indeterminate gradient for the ideal magnets, is replaced by a more realistically gradual curve. This curve bridges the types 1 and 2 behaviour and identifies a new, type T behaviour.

Sets of fabricated magnets can be classified with the $Y = KX^L$ equation according to the values of K and L, the constants of fit. K and L can separately range from 0 to 1. However, it is the sum, $K + L$, that we find most useful for the purpose of classification. The various ranges of $K + L$ and the corresponding type of ferromagnet sets described are summarised in Table I. For type 2 curves the condition, $K + L = 1$, is particularly simple. We may, therefore, calculate expected type 2 curves for any combination of K and L which sums to unity. Calculated examples of type 2 curves are shown in Fig. 2. Similarly, it is possible to calculate the curves corresponding to type T and the mixed types 1-T and T-2 ferromagnet sets from the approriate $K + L$ values. Finally, we note the remaining condition of $0 < K + L < 1$. The curves defined by this sum appear to arise from the (X, Y) values of

TABLE I The classification of ferromagnets according to ranges of the $(K + L)$ values

$(K + L)$ range	Ferromagnet type	Comment
$0 < K + L < 1$	Type 2 magnets	Magnets not forming set (see text). Becker type 2
$K + L = 1$	Type 2 set	Becker type 2
$1 < K + L < 1.25$	Types 2-T overlap	
$1.25 < K + L < 1.75$	Type T	$0 < K < 1$ $0 < L < 1$ Type T condition
$1.75 < K + L < 2$	Types T-1 overlap	
$K + L \sim 2$	Type 1	$K \sim L \sim 1$ Becker Type 1

magnets which are individually type 2, but do not form a set as defined by the above provisions, (a) to (c). Hence these curves intersect the $K + L = 1$, type 2 curves.

3. The $Y = KX^L$ equation fitted to empirical data

Empirical data for a number of SmCo and Nd–Fe–B based magnet sets have been analysed and fitted to the $Y = KX^L$ equation. Results from this analysis are summarized in Tables II–IV, the magnet sets having been chosen to examplify different types, corresponding to various $K + L$ combinations. Major process details and physical variables along the $(X < Y)$ curves are also included in the tables for each of the magnet sets. This inclusion stresses the view that the (X, Y) classification can be applied to the actual fabricated magnet sets and not merely to the basic ferromagnetic materials themselves. Taking into account that the data used for a number of sets were merely read from published graphs, it is remarkable that good $Y = KX^L$ fits have been obtained for the variety of materials, process and measurement conditions represented here. It is also notable that the $K + L$ sum for each of the three magnet sets in Table II is within 2% of the unity value expected for their classification as Type 2. These type 2 curves can be visualized by interpolation within the calculated graphs in Fig. 2.

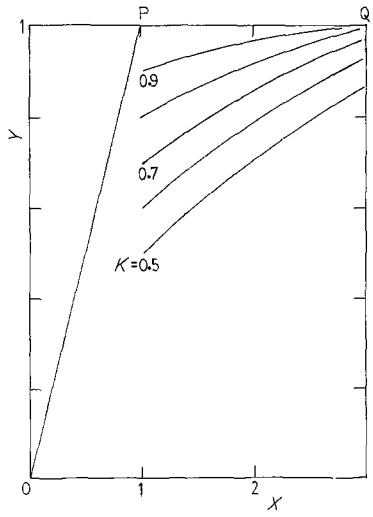

Figure 2 Calculated $Y = KX^L$ curves for Type 2 $(K + L = 1)$ ferromagnet sets; $K = 0.5$, 0.6, 0.7, 0.8 and 0.9.

TABLE II Examples of Type 2 ($K + L = 1$) rare earth ferromagnet sets

Magnet set [Ref]	Major process details	K, L	Range B_r (kG)	Primary variables along curve
$SmCo_x$: M(F)	Milled powder,	0.567	2.76 to 5.24	$4.8 \leqslant x \leqslant 5$
[1, 2]	cold set polymer	0.432		Particle size
$SmCo_x$: HD(F)	Hydrided powder,	0.727	4.25 to 5.66	$4.8 \leqslant x \leqslant 5$
[2]	cold set polymer	0.259		Particle size
Nd–Dy–Fe–B	Sintered, heat	0.895	10.95 to 12.4	Dy content (refer
[4]	treated	0.117		to [4] for details)

The fitted curves corresponding to Tables III and IV are shown respectively in Figs 3 and 4.

4. Discussion of empirical data fitted to $Y = KX^L$

The sets of fitted data in Tables II–IV can be seen to correlate to the main characteristics of the three types of magnet sets, according to the Becker conditions plus the type T condition and also the respective $K + L$ combinations specified in this paper. For the rare earth based magnets, the type 1 classification is of no consequence and so we shall only need to discuss here the details of correlation to types T and 2.

4.1. Sintered and polymer bonded magnets

The most notable feature of the magnet sets in Table IV, for which the $K + L$ ranges apply to types T and T-1 overlap, is that they are all sintered. Effects of sintering include densification and grain growth in the sintered magnet. The consequences of these effects are, usually, an increase in Br accompanied by decreased coercivities, features of a type T character. In contrast, cold set polymer bonding of aligned magnetic powder will not significantly affect any densification and the starting powder particles will therefore remain as separate entities in the fabricated magnet. Therefore these magnets will have relatively low remanence values but can have enhanced coercivities, which are features of a type 2 character.

4.2. Dysprosium substitution of neodymium in Nd–Fe–B based magnets

Besides the two SmCo based polymer bonded sets discussed above, Table II also include a Nd–Fe–B based sintered set in which there is a successive substitution of neodymium by dysprosium [4]. This contrasts with the purely Nd–Fe–B sintered set [9] in Table IV, where the empirical variable is merely the relative neodymium content. Although Ma and Krause [9] also studied in detail sintered NdDyFeB magnets, the data for these magnets are not suitably reported for our present analysis. However, they point out that the substitution of dysprosium for neodymium improves the intrinsic coercivity of the basic Nd–Fe–B magnets by (i) the fundamental effect of increasing the anisotropy field as well as (ii) the process related consequence of grain growth inhibition during sintering and high temperature ageing. Hence the effect on the (X, Y) graph due to the dysprosium substitution of neodymium may still tend to be characteristic of a type 2 classification, even though the magnets have been sintered and subjected to a high temperature ageing treatment.

Finally, we note that increasing the temperature at which the magnetic properties of fabricated Neomax 30-H and 35 magnets are measured [8] causes reductions in the remanences and, even more rapidly, in the coercivities. The reductions in all the magnetic parameters with temperature were less rapid for the 30-H set than with the 35 set. According to our analysis here, the 30-H set has a $K + L$ sum that is type T bordering on the type T-2 overlap while that for the 35 set is within the type 1-T overlap range. This observation is consistent with the above discussion on the effects of dysprosium in Nd–Fe–B magnets since the 30-H set is stated to have "a small dysprosium addition" [8].

4.3. The types T-2 overlap range

From the above discussion that the ideal limits of the $Y = KX^L$ curve are the straight lines OP and PQ (Fig. 1), we can expect that the fitting of type T-2 overlap data will be complicated by the indeterminate gradient at the point P. Although reasonably good fits have been obtained for the magnet sets considered here (Table III and Fig. 3), it may prove even more useful to fit the empirical data in two groups instead, with the separation at $X = 1$. Alternatively, more terms can be included in the equation of fit to accommodate a less gradual gradient variation in the vicinity

TABLE III Examples of Types 2-T overlap ($1 < K + L < 1.25$) rare earth ferromagnet sets

Magnet set [Ref]	Major process details	K, L	Range B_r (kG)	Primary variables along curve
$SmCo_x$: HD(A)	As HD(F),	0.709	4.25 to 5.86	$4.8 \leqslant x \leqslant 5$
[2]	Table II, aged	0.371		Particle size
$SmCo_5$	Compacted and	0.638	7.8 to 9.5	Sinter
[5]	sintered	0.481		temperature
				Density
$SmCo_x$: M(A)	As M(F),	0.543	2.77 to 5.27	$4.8 \leqslant x \leqslant 5$
[2]	Table II, aged	0.596		Particle size
$SmCo_5$	Thermoplastic	0.509	5.2 to 6.4	Particle size
[6]	bonded	0.737		

TABLE IV Examples of Type T ($1.25 < K + L < 1.75$) and types T-1 Overlap ($1.75 < K + L < 2$) rare earth ferromagnet sets.

Magnet set [Ref]	Major process details	K, L	Range B_r (kG)	Primary variables along curve
$SmCo_5$	Sintered	0.667	8.2 to 9.5	$4.69 \leqslant x \leqslant 5.16$
[7]		0.642		Particle size
Neomax 30-H	Sintered	0.736	9.2 to 12.4	Temperature
[8]	Nd–Fe–B based	0.642		(20–200° C)
Neomax 35	Sintered	0.851	9.2 to 12.2	Temperature
[8]	Nd–Fe–B based	0.909		(20–200° C)
NdFeB	Sintered High T	0.851	10.8 to 12.5	Nd content; Density;
[9]	aged	0.949		Microstructure (see Ref. for details)

of $X = 1$. Examples or other sets of data that may require a similar re-analysis are the sintered $SmCo_x$ and Neomax 30-H sets in Table IV (graphs a and b respectively in Fig. 4). In this case, the ranges of $K + L$ which correspond to types T-2 overlap and type 2 classification may need to be respecified. A more detailed discussion of these aspects, together with the analysis of additional magnet sets for which suitable data is available, will be reported in a future paper.

5. Conclusions

(1) The usefulness of the $Y = KX^L$ equation for the classification of ferromagnetic materials has been analysed further.

(2) A major conclusion of this analysis is that the Becker classification of ideal (square demagnetization loop) ferromagnets into two types should be extended, for fabricated magnet sets, to include a third, intermediate type.

(3) Regimes for the different types and type overlaps are identified with corresponding combinations of $K + L$.

(4) Comparison with empirical data for a number of rare earth based magnet sets has shown that the present graphical scheme is useful, not only for the classification of basic ferromagnetic materials, but also of composition substitutional effects, fabrication processes and measurement conditions.

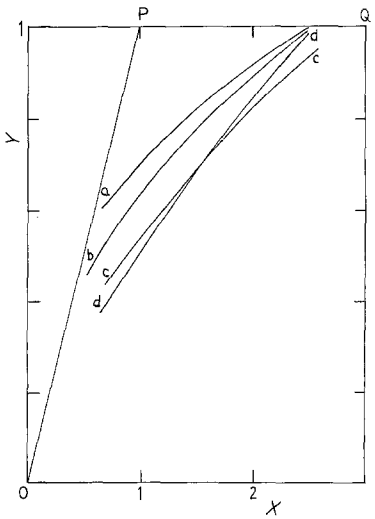

Figure 3 Fitted $Y = KX^L$ curves for the Types 2-T overlap rare earth ferromagnet sets in Table III; (a) $SmCo_x$: HD(A), (b) $SmCo_5$: sintered, (c) $SmCo_x$: M(A), (d) $SmCo_5$: thermoplastic bonded.

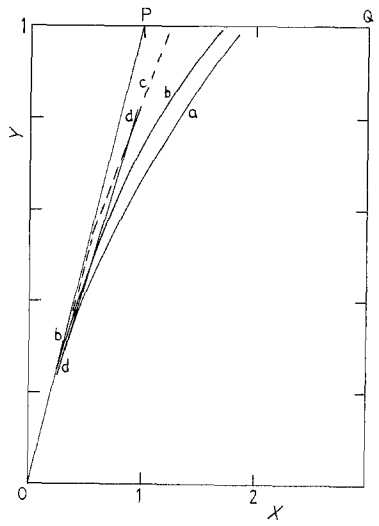

Figure 4 Fitted $Y = KX^L$ curves for the type T and types T-1 overlap rare earth ferromagnet sets in Table IV; (a) $SmCo_x$: sintered, (b) Neomax 30-H, (c) Neomax 35, (d) NdFeB.

Acknowledgement

Helpful discussions with I. R. Harris, N. Rowlinson and P. Withey are acknowledged. I am grateful to Professor R. E. Smallman for use of the facilities in the Department of Metallurgy and Materials, University of Birmingham.

References

1. C. Y. TAY and I. R. HARRIS, *J. Mater. Sci. Lett.* **4** (1985) 114.
2. *Idem, ibid.* **5** (1986) 214.
3. J. J. BECKER, *Trans. IEEE Magn. Mag.* **4** (1968) 239.
4. M. TOKUNAGA, N. MEGURO, M. ENDOH, S. TANIGAWA and H. HARADA, *ibid.* **21** (1985) 1964.
5. K. S. V. L. NARASIMHAN and T. LIZZI, *J. Appl. Phys.* **57** (1985) 4158.
6. K. KAMINO and T. YAMANE, *Goldschmidt Informiert* **2/79** (1979) 23.
7. D. L. MARTIN, M. G. BENZ and A. C. ROCKWOOD, AIP Conference Proceedings, Vol. 10, (edited by C. D. Graham Jr and J. J. Rhyne) American Institute of Physics, New York (1973) p. 583.
8. D. LI, H. F. MILDRUM and K. J. STRNAT, *J. Appl. Phys.*, **57** (1985) 4140.
9. B. M. MA and R. F. KRAUSE, Proceedings 5th International Symposium on Anisotropy and Coercivity in Rare-Earth Transition Metal Alloys, Bad Soden, FRG, Aug. 31–Sept. 2, 1987 Deutsche Physikalische Geselschaft, Bad Honnef, FRG (1987) p. 141.

Received 8 January
and accepted 9 May 1988